



Low-frequency sound transmission loss of honeycomb metastructure with in-parallel arrangement of Helmholtz resonators

Denilson Ramos¹, Luis Godinho¹, Paulo Amado-Mendes¹, Paulo Mareze²

¹University of Coimbra, ISISE, Department of Civil Engineering
dtramos@student.dec.uc.pt, lgodinho@dec.uc.pt, pamendes@dec.uc.pt

²Federal University of Santa Maria, Department of Structures and Civil Construction, Acoustic Engineering
paulo.mareze@eac.ufsm.br

Abstract

Resonators can be effective devices to help to tackle low-frequency insulation, and have been widely investigated in the literature. In building acoustics, literature reports their historical use, leading to the design of new structures for room acoustic optimization, and urban and environmental mitigation. Structures based on sub-wavelength resonances are an ideal solution for the development of thin absorbent materials matching the specific impedance with the background medium. In this work, analytical solutions describing acoustic wave propagation in ducts coupled with the transfer matrix method are used to predict the sound attenuation characteristics of a subwavelength metastructure. Its accuracy is validated by a finite element model. The preliminary results presented in this work show the improvement capacity of this system when geometric parameters are studied, exhibiting a significant response in the properties of sound transmission loss (STL).

Keywords: Acoustic Metamaterials, resonators, sound insulation, low-frequency, sound transmission loss.

1 Introduction

In acoustics, the frequent interest in the manipulation of acoustic energy in subwavelength regimes has led to continuous advances in the science of metamaterials, namely acoustic metamaterials (AMM), whose applicability presents physical characteristics in ways not seen in ordinary acoustic materials [1].

The class of AMM that comprises the inclusion of resonant structures, as firstly evidenced by Fang et al. [2], leads to effective physical properties, determined by their structures to the detriment of their constituent materials.

The resonant nature of these mechanisms offers important contributions to the field of developing subwavelength structures, with great capacity sound absorption and transmission characteristics, with ample potential to be explored in passive building ventilation systems, providing guaranteed air circulation, thermal comfort and reducing the effects of noise pollution on human health [3].

Considering the airborne noise attenuation, the application of acoustic barriers, as a common noise mitigation strategy, tends to face limitations, requiring an increase in the layer thickness, to act in low-frequency regimes. In this sense, subwavelength resonant structures provide a viable solution for the development of thinner absorbent materials, dealing with audible frequencies below 1kHz [4], as well as the development of new structures, allowing some air passage.

The literature has presented several types of research based on the noise mitigation capability of simple or clustered resonant structures, leading to interesting responses to effective parameters with an emphasis on

airflow. In turn, Jena et al. [5] investigated eight configurations of Helmholtz resonators (HR), in parallel and serial arrangements, with similar and different resonators, going beyond the propositions of AMM with the idea of in-line coupling. From these investigations, it was observed that five finite matrix configurations exhibit a negative effective mass density and negative mass modulus. Kumar et al [6], presented an effective negative bulk modulus, leading to transmission loss at normal incidence of up to 18 dB, ensuring a ventilation area of 45%.

Kim and Lee [7], based on the theory of sound diffraction and metamaterials as a negative bulk modulus, propose a transparent acoustic barrier system consisting of a three-dimensional matrix of resonators, with satisfactory performance levels for frequencies from 700 to 2200 Hz. Jung et al.[8], presented a panel, designed to attenuate noise in the audible band with its absorption mechanism due to the matrix of annular cavities, leading to a negative bulk modulus.

However, these devices may not provide broadband attenuation due to features such as bulky size and the need for an extra area for deployment. Another issue is the relationship between noise attenuation and airflow passage: when a larger area of ventilation is considered, smaller sound transmission is usually registered.

In this sense, the option of applying Helmholtz resonators, as tunable devices, already widely theorized for sound attenuation, in subwavelength dimensions, still presents itself as a viable strategy mainly due to the advances in new additive manufacturing techniques, enabling the inclusion of a greater number of resonant units, reaching higher frequency bands, with an emphasis on passive airflow.

In this study, the authors propose a simplified model for predicting acoustic properties of AMM based on locally resonant inclusions, through analytical models [9], [10], taking into account the viscous thermal losses within the boundary layer. Subsequently, the transfer matrix method [11] is used to analyze the plane wave propagation through the proposed metamaterial, investigating the transmission loss as an acoustic parameter to verify the device's performance. A finite element model is then implemented to verify the usefulness of the model and then present the correlation between theoretical and numerical models for STL, evidencing good agreements between the models.

This work is organized as follows: in section 2, the authors propose a theoretical prediction model for modeling wave propagation in narrow ducts, extending the classical theory of HR for application in acoustic metamaterials, analyzing the sound transmission of these, based on the transfer matrix method. In section 3, the validation of the proposed theoretical model is presented, comparing the predictions considering the losses dissipation that occurs in sound transmission with finite element simulations. Finally, the theoretical models presented will be discussed, with the main conclusions summarized in section 4.

2 Theory

2.1 The theoretical model for sound waves propagation in narrow tubes

Understanding the sound wave propagation in a narrow and uniform tube is a fundamental problem in acoustic material science. The study of sound propagation in narrow ducts, as in Helmholtz resonators, takes into account the viscous thermal losses, arising from air friction and its interaction at the limit of the solid boundary inside the duct, having a relationship dependent on the channel ratio [12].

Several theoretical prediction models provided [9], [10] take into account the effects of air viscosity and thermal conductivity in tubes from narrow to arbitrary dimensions. This energy dissipation can be theoretically obtained through the equivalent mass density $\rho_i^{[n]}$ and the equivalent bulk modulus $\kappa_i^{[n]}$ of the narrow duct, expressed by [9], [13], [14]:

$$\rho_i^{[n]} = - \frac{\mu w_i^4}{4j\omega \sum_{t=0}^{\infty} \sum_{m=0}^{\infty} (x_t^2 y_m^2 (x_t^2 + y_m^2 - j\omega\rho_0/\mu))^{-1}}, \quad (1)$$

$$\kappa_i^{[n]} = - \frac{\mu \kappa_0 w_i^4}{\gamma \mu w_i^4 + 4(\gamma - 1) P_r \rho_0 \omega \sum_{t=0}^{\infty} \sum_{m=0}^{\infty} (x_t^2 y_m^2 (x_t^2 + y_m^2 - j \omega P_r \rho_0 / \mu))^{-1}} \quad (2)$$

where i represents the respective value for tubes in different sections, such as the neck and cavity of a Helmholtz Resonator; $\omega = 2\pi f$ is the angular frequency, $\rho_0 = 1.213 \text{ kg} \cdot \text{m}^{-3}$ is the density of air, $\mu = 1.84 \times 10^{-5} \text{ N} \cdot \text{s} \cdot \text{m}^{-2}$ the dynamic viscosity of air, $P_r = 0.707$ is the Prandtl number; $\gamma = 1.4$ is the ratio of specific heat; $\kappa_0 = 1.42 \times 10^5 \text{ Pa}$ is the bulk modulus of air.

Considering the geometric parameters, w_i corresponds to the dimensions of a duct, w_n and w_c the dimensions of the neck and cavity of an HR, respectively. Thus, the terms $x_t = (t + 1/2)\pi/w_i$, $y_m = (m + 1/2)\pi/w_i$, with t and m being positive integers. Hence, the effective wavenumber and acoustic impedance are given by $k_i^{[n]} = \omega \sqrt{\rho_i^{[n]}/\kappa_i^{[n]}}$ and $Z_i^{[n]} = \sqrt{\kappa_i^{[n]} \rho_i^{[n]}/w_i^2}$, respectively.

In Figure 1, the proposed axial acoustic metamaterial consists of N generic resonators, where, $l_n^{[n]}$ corresponds to the length of the resonator's neck, $w_{n,1}^{[n]}$ and $w_{n,2}^{[n]}$ corresponds to the dimensions of the neck opening with a rectangular section, $l_c^{[n]}$ corresponds to the length of the resonator cavity, $w_{c,1}^{[n]}$ and $w_{c,2}^{[n]}$ correspond, respectively, to the dimensions of the rectangular section cavity. For simplification purposes, the central hole corresponds to a circumscribed hexagon S_h with radius r_h .

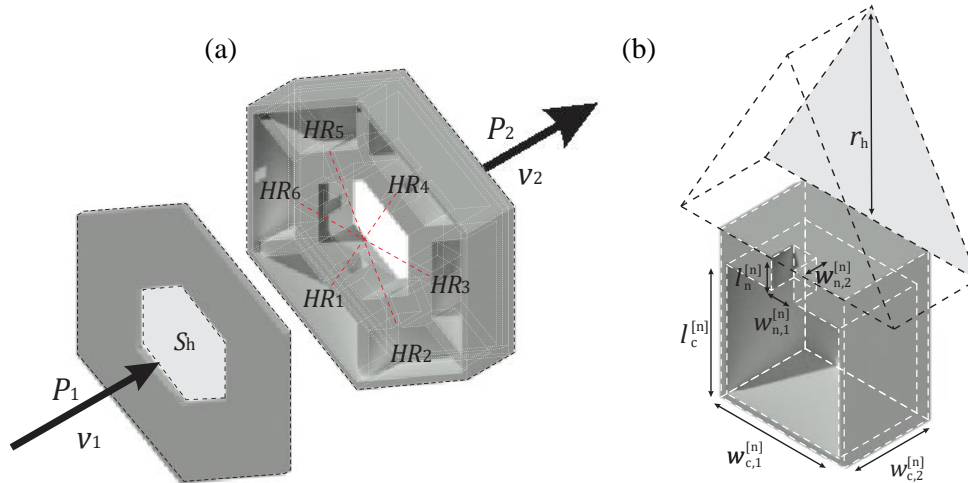


Figure 1 – Conceptual diagram of the proposed acoustic metamaterial. (a) Scheme of the unit cell composed of a set of N in-parallel Helmholtz Resonators, embedded in an open area (airflow passage). (b) An equivalent HR of the metamaterial for theoretical analysis.

Thus for an HR coupled to a waveguide, Figure 1(b), its characteristic effective impedance can be expressed as [15]–[17],

$$Z_{HR}^{[n]} = -i \frac{\cos(k_n l_n) \cos(k_c l_c) - Z_n k_n \Delta l \cos(k_n l_n) \sin(k_c l_c) / Z_c - Z_n \sin(k_n l_n) \sin(k_c l_c) / Z_c}{\sin(k_n l_n) \cos(k_c l_c) / Z_n - k_n \Delta l \sin(k_n l_n) \sin(k_c l_c) / Z_c + \cos(k_n l_n) \sin(k_c l_c) / Z_c} \quad (3)$$

$k_n^{[n]}$, $k_c^{[n]}$, correspond to the complex wave number vector, for the neck and cavity, respectively; $Z_n^{[n]}$, $Z_c^{[n]}$, correspond to the specific impedance characteristic of the segments.

When considering the lateral coupling of the HR in a waveguide of the circular section of arbitrary radius, r_t ; the sound radiation correction factor, Δl , expresses the interface discontinuity between the waveguide and the resonator neck, corresponding to the addition of the two length correction factors $\Delta l = \Delta l_1^{corr} + \Delta l_2^{corr}$, being expressed by [13],

$$\Delta l_1^{corr} = 0.82 \left[1 - 1.35 \left(\frac{w_n^{[n]}}{w_c^{[n]}} \right) + 0.35 \left(\frac{w_n^{[n]}}{w_c^{[n]}} \right)^3 \right] w_n^{[n]}, \quad (4)$$

$$\Delta l_2^{corr} = 0.82 \left[1 - 0.235 \left(\frac{w_n^{[n]}}{r_t} \right) - 1.32 \left(\frac{w_n^{[n]}}{r_t} \right)^2 + 1.54 \left(\frac{w_n^{[n]}}{r_t} \right)^3 - 0.86 \left(\frac{w_n^{[n]}}{r_t} \right)^4 \right] w_n^{[n]}. \quad (5)$$

The first correction, Δl_1^{corr} , corresponds to the sound wave radiation and the interface discontinuity between the neck sections, $w_n^{[n]}$, to the resonator cavity section, $w_c^{[n]}$; while the second correction Δl_2^{corr} , corresponds to the discontinuity between the radius waveguide, r_t , and the radius of resonator neck, $r_n^{[n]}$ [13], [15], [17].

2.2 Transfer matrix formulation for sound transmission loss

The transfer matrix method (TMM) in a finite duct corresponds to the propagation of the plane wave, under the condition of continuity of sound pressure and particle velocity, in an acoustic system coupled to a waveguide segment, with a length l_{tube} , and r_{tube} the respective radius of the cross section [11].

The application of the theoretical models proposed above can be used through the TMM; just assume the continuity of sound pressure, p , and normal particle acoustic velocity, v , from the beginning to the end of the system, with only the propagation of plane waves in the waveguide, the transfer matrix, \mathbf{T} can be derived. The relationship between incident sound pressure and particle velocity from an initial moment, p_1 and v_1 , respectively, to the final moment p_2 and v_2 , being written as[5], [18],

$$\begin{bmatrix} p_1 \\ v_1 \end{bmatrix} = \begin{bmatrix} T_{11} & T_{12} \\ T_{21} & T_{22} \end{bmatrix} \begin{bmatrix} p_2 \\ v_2 \end{bmatrix} = \mathbf{T} \begin{bmatrix} p_2 \\ v_2 \end{bmatrix}. \quad (6)$$

Taking into account n resonators coupled to a waveguide expressed by the matrix $\mathbf{M}_{HR}^{[n]}$, and the radiation in a circular waveguide, expressed by $\mathbf{M}_{tube}^{[n]}$, take the form $\mathbf{T} = \mathbf{M}_{tube}^{[n]} \mathbf{M}_{HR}^{[n]} \mathbf{M}_{tube}^{[n]}$, where the transfer matrix for the resonator and tube are expressed, respectively, by [19],

$$\mathbf{M}_{HR-i}^{[n]} = \begin{bmatrix} 1 & 0 \\ 1/Z_{HR-i}^{[n]} & 1 \end{bmatrix}, \quad (7)$$

$$\mathbf{M}_{tube}^{[n]} = \begin{bmatrix} \cos(kl) & iZ_0 \sin(kl) \\ i \sin(kl) / Z_0 & \cos(kl) \end{bmatrix}. \quad (8)$$

where $Z_{HR}^{[n]}$ is the impedance of the n -th resonator, k is the wavenumber in the air and $Z_0 = \rho_0 c_0 / S_{tube}$, is to the characteristic impedance of the waveguide.

Due to the resonance characteristics of the Helmholtz resonator, its response is centered on a narrow frequency band. Thus, to widen the frequency band, achieving a hybrid control, a system of n laterally coupled Helmholtz resonators (for the metamaterial presented here $n = 6$) in the same cross-section, under conditions of propagation, a plane wave is considered, and the total impedance of the AMM presented can be expressed as,

$$Z_{metastructure} = \sum_{n=1}^n 1/Z_{HR-i}^{[n]}. \quad (9)$$

The transfer matrix for the meta structure follows the form,

$$\begin{bmatrix} p_1 \\ v_1 \end{bmatrix} = \begin{bmatrix} 1 & 0 \\ (Z_{metastructure}) & 1 \end{bmatrix} \begin{bmatrix} p_2 \\ v_2 \end{bmatrix}. \quad (10)$$

Therefore, the sound transmission presented by the system in parallel is given by,

$$TL = 20 \log_{10} \left(\frac{1}{2} |T_{11} + T_{12}/Z_0 + T_{21} Z_0 + T_{22}| \right). \quad (11)$$

Through the above equation, it is evident that the sound transmission is dependent on the individual resonances of the resonators, therefore, through geometric alteration, the changes in the resonant frequencies lead to interesting results, reaching a wider band as observed in the following section.

3 Results

3.1 Comparison between theoretical and numerical models

The inclusion of subwavelength resonant units is studied through a finite element model conducted using the commercial software COMSOL multiphysics. Considering the results obtained, these will be compared with theoretical values to verify the accuracy between the models presented.

In Figure 2, assuming the periodicity condition imposed in the model, under the action of a plane wave of unitary value at normal incidence originated in a sound hard boundary, the waveguide and the AMM surfaces were considered as perfectly rigid surfaces, having all internal domains computationally modeled as air; to mitigate subsequent reflections, a perfectly matched layer (PML) is admitted at both ends of the waveguide. To verify and approximate the results, viscous thermal losses in narrow domains (neck of the resonator) were considered, dealing with the dissipation of acoustic energy inside the boundary layer.

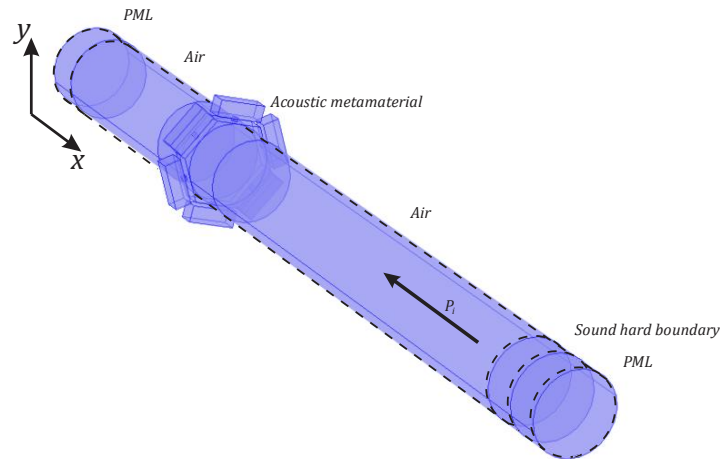


Figure 2 – Schematic view of the numeric model of the proposed AMM with a waveguide.

For analysis and comparison of the proposed models, both the theoretical prediction (as presented in section 2) and the numerical model take into account the viscous-thermal dissipation. To verify the main contributions and possible differences between models, the effect of the geometric parameters $w_n^{[n]}$ and $l_n^{[n]}$ is here evaluated, since they are the main parameters to be considered in the dissipative loss of acoustic energy inside the boundary layer that influence the TL of the acoustic metamaterial.

First, we analyze the behavior of the meta unit tuned to the same frequency. Let us consider a first meta-structure with the axial coupling of 6 HRs. The geometric parameters corresponding to each resonator are set as, $l_c^{[n]} = 40$ mm, $l_n^{[n]} = 5$ mm, and, $w_{c,1}^{[n]} = w_{c,2}^{[n]} = 20$ mm. The central hexagon hole radius $r_h = 15$ mm.

We varied the neck size in $w_{n,1}^{[n]} = w_{n,2}^{[n]} = 2$ mm, for the first model, having as resonance frequency $f_{r1} = 290$ Hz; for the second model at $w_{n,1}^{[n]} = w_{n,2}^{[n]} = 3$ mm, with a resonant frequency $f_{r2} = 410$ Hz; and finally, in $w_{n,1}^{[n]} = w_{n,2}^{[n]} = 4$ mm, with a resonant frequency $f_{r3} = 680$ Hz.

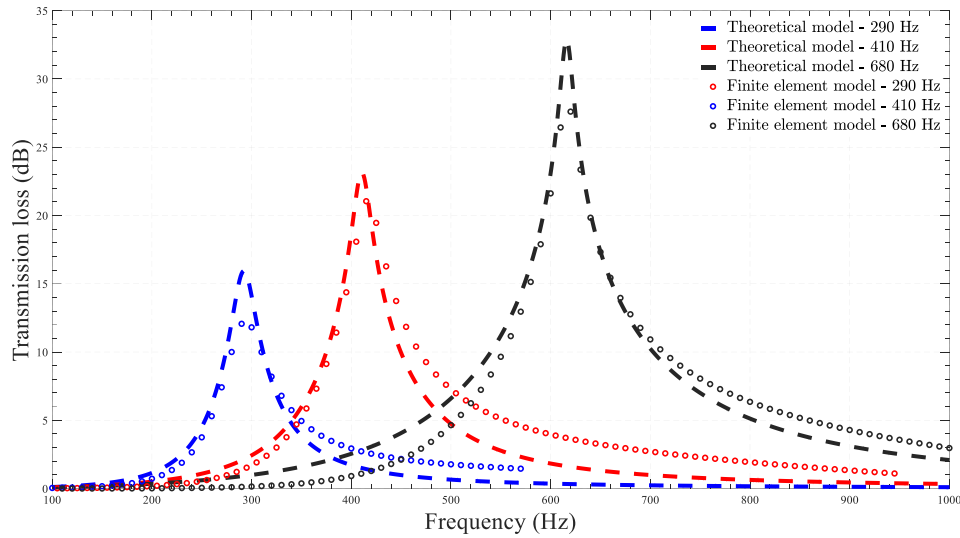


Figure 3 – The sound transmission loss spectrum for the hexagonal metamaterial model composed of HR tuned to the same frequency, varying only the geometric parameter $w_n^{[n]}$. Dots correspond to the proposed theoretical model and Dashed lines to the applied numerical model, taking into account viscous thermal losses. In blue, the tuned structure corresponds to the 290 Hz; red lines correspond to HR tuned to 410 Hz; in black, the lines correspond to the AMM resonant frequency of 610 Hz.

In Figure 3, the dots correspond to the predicted numerical values, while the dashed lines refer to the analytical results for the STL of the metamaterial presented here. From Figure 3, for STL values, it is possible to observe peak values for sound transmission loss of 15 dB, 23 dB, and 32 dB for analytical results while 12 dB, 21 dB, 27 dB are computed for numerical values, respectively for frequencies of 290 Hz, 410 Hz, and 610 Hz. It can be seen that there is good agreement between the predictions associated with both approaches considering the models presented, in a situation of normal incidence.

Given the possibility of variations due to dissipative losses, next, we investigate the contributions from the geometric parameter $l_n^{[n]}$, at the boundary of the inner layer, comparing also theoretical and numerical results.

In this case, the geometric parameters corresponding to each resonator are set as, $l_c^{[n]} = 40$ mm, $w_{c,1}^{[n]} = w_{c,2}^{[n]} = 20$ mm, the neck dimension $w_{n,1}^{[n]}$ and $w_{n,2}^{[n]}$, are fixed at 5 mm. The central hexagon hole radius $r_h = 15$ mm. We varied the neck length of the first model, $l_{n1}^{[n]} = 20$ mm, with a resonance frequency $f_{r1} = 410$ Hz; for the second model, the dimension is $l_{n2}^{[n]} = 10$ mm, having a resonance frequency $f_{r2} = 515$ Hz; and, finally, for the third model, the dimension is $l_{n3}^{[n]} = 5$ mm, presenting a resonant frequency $f_{r3} = 615$ Hz.

For the predictions and comparison of the proposed models, in Figure 4, for STL values, it is possible to observe values for sound transmission loss of 27 dB, 30 dB, and 32 dB for analytical results while 21 dB, 28 dB, 33 dB are obtained for the numerical model, respectively for the frequencies of 410 Hz, 515 Hz, and 615 Hz, it can be seen that there is good agreement between the predictions associated with both approaches considering the models presented, in a situation of normal incidence.

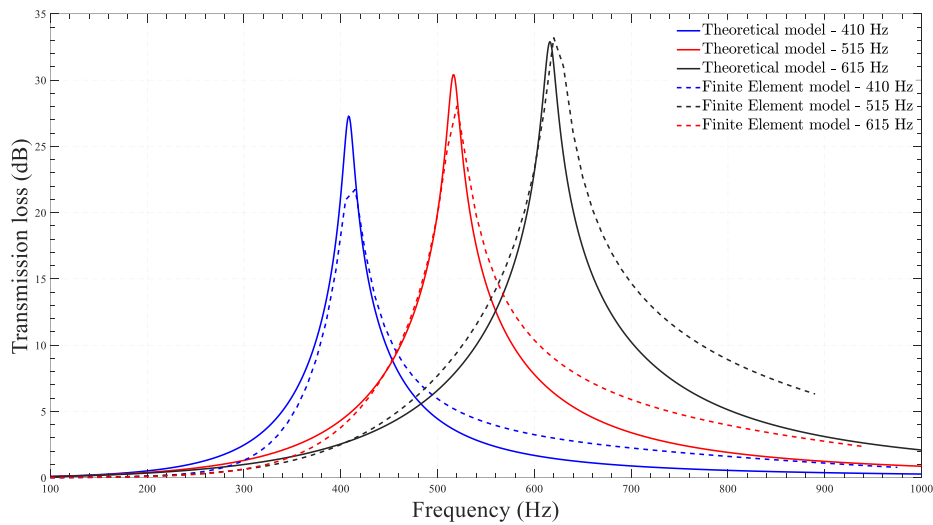


Figure 4 – The sound transmission loss spectrum for the hexagonal metamaterial model composed of HR tuned to the same frequency, varying only the geometric parameter $l_n^{[n]}$. Solid lines correspond to the proposed theoretical model and dashed lines to the applied numerical model, taking into account viscous thermal losses. In blue, the tuned structure corresponds to the 410 Hz frequency; red lines correspond to HR tuned to 515 Hz frequency; in black, the lines correspond to the AMM resonant frequency of 615 Hz.

The results reveal the dependence of thermo-viscous losses inside the boundary layer for the resonator neck as a conditioning factor for the agreement between the results. From our analysis, it seems that way in which the thermal-viscous losses are included as well as the correction factors at the neck and waveguide interface, are the main responsible for the differences between the proposed models, since the STL amplitude presents a good correlation between all models. Thus, in general, the proposed theoretical models present acceptable agreement with the model based on the finite element method for the proposed AMM.

3.2 Performance observation

In this subsection, the performance of the proposed AMM is evaluated, now considering the coupling of HR with different frequencies of resonance. In the case of reaching a wide frequency range per meta unit, we analyse the case of grouping resonant structures with different resonance frequencies, based on the geometric change of the proposed models.

Considering the parallel arrangement of N Helmholtz resonators grouped in the same cross-section of a waveguide, as illustrated in Figure 1, and the acoustic impedance of this structure can be calculated theoretically as expressed in equation 9.

The predicted transmission loss for the AMM considering a set of three groups with different resonant frequencies formed by 2 HR each, with pairs always positioned on the opposite side is shown in Figure 5.

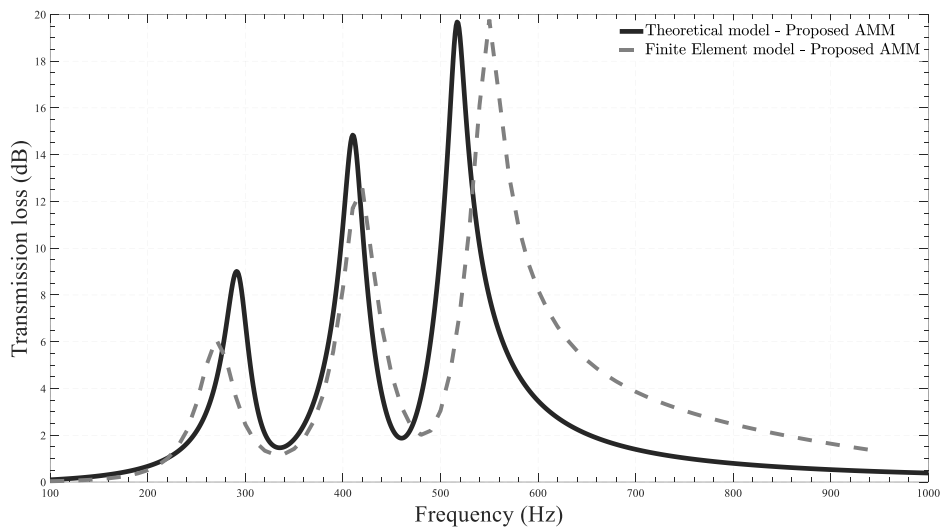


Figure 5 – The AMM for three resonance frequencies. The spectrum of sound transmission loss for the meta unit cell with every two HRs tuned for specific resonance frequencies allowing three peaks for attenuation. Comparison between the numerical (dashed line) and theoretical (solid line) TL with three resonant frequencies at 290 Hz, 410 Hz, and 520 Hz.

The solid line represents the STL for the proposed meta-unit with HR tuned to 3 resonance frequencies. As shown, approximately 20 dB transmission loss is observed at a frequency of approximately 500Hz; however, it is evident that the peak attenuation only happens at the frequencies to which the system is tuned, and a significant drop is seen between the resonant frequencies. From the theoretical and numerical models, good agreements can be observed at the lower resonances, although a visible deviation is seen for the higher resonant frequency.

Figure 6 presents the sound transmission loss based on the in-line coupling of the metamaterials proposed previously in Figure 3 and Figure 4. In the model, only the analysis based on the finite element method was considered.

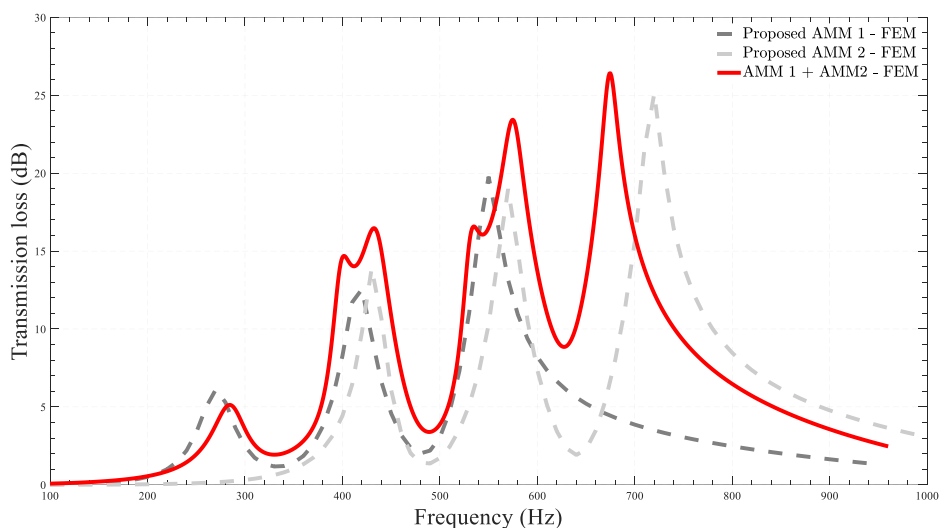


Figure 6 – The spectrum of sound transmission loss for the coupling of two meta unit cells with three resonant frequencies each one; the dashed lines in gray corresponds to the individual TL capacity of each AMM.

A FEM simulation is used to investigate the sound attenuation capacity of the serial coupling of two proposed meta structures. The red line corresponds to the proposed serial coupling of two AMM; for this model an STL peak of up to 25 dB can be observed, for frequencies of 590 Hz and 680 Hz; for this structure, it is observed that the serial coupling has the potential to increase the magnitude of TL between the frequencies of interest, reducing the observed gap. The predicted results of the transmission loss through multiple resonators mounted inside branch arrangement allowed observing significant changes in the noise attenuation of the system due to this well-known resonance principle. The arrangements shown here can be applied in the design of noise attenuation devices tuned in multiple frequencies with different TL magnitudes, leading to efficient devices.

4 Conclusions

In this work, the authors analyzed the development of a subwavelength acoustic metamaterial, consisting of the axial coupling of n Helmholtz resonators. The parallel grouping of resonant units at different frequencies is presented as a strategy to achieve greater bandwidth, while also ensuring a reduced thickness of the structure.

The investigation of the influence of the dissipation of acoustic energy was also performed, through variation of the dimensions of the length of the neck and the cross-sectional area of an HR, indicating good agreement when comparing the theoretical and numerical models.

Considering the main objective of the work, the behavior of the STL has been analyzed for AMM configurations, considering the parallel coupling of HRs, guaranteeing different frequency peaks and considerable performance. The transmission loss achieved by a periodical HR system is dependent on the structure and number of HRs, as well as its geometric parameters, considering its relationship with the dimension of the opening of the air passage.

In future works, the aim is to study the application of the proposed acoustic metamaterial to increase and widen the sound attenuation band, based on serial coupling, as well as the possibility of studying such effects in physical prototypes in experimental tests. It is expected that the present study can serve as an important contribution to the research and development of AMM with applications in sound attenuator systems that enable airflow in the diverse applications in engineering.

Acknowledgments

This work is financed by national funds through FCT - Foundation for Science and Technology, under grant agreement UI/BD/150864/2021 attributed to the 1st author, and by FCT/MCTES through national funds (PIDDAC) under the R&D Unit Institute for Sustainability and Innovation in Structural Engineering (ISISE), under reference UIDB / 04029/2020.



References

- [1] S. A. Cummer, J. Christensen, and A. Alù, Controlling sound with acoustic metamaterials, *Nature Reviews Materials*, vol. 1, no. 16001, pp. 1–14, 2016.
- [2] N. Fang *et al.*, Ultrasonic metamaterials with negative modulus, *Nature Materials*, vol. 5, no. 6, pp. 452–456, Jun. 2006.
- [3] M. H. F. De Salis, D. J. Oldham, and S. Sharples, Noise control strategies for naturally ventilated buildings, *Building and Environment*, vol. 37, no. 5, pp. 471–484, May 2002.

- [4] S. Kumar and H. P. Lee, Recent advances in acoustic metamaterials for simultaneous sound attenuation and air ventilation performances, *Crystals*, vol. 10, no. 8, pp. 1–22, 2020.
- [5] D. P. Jena, J. Dandsena, and V. G. Jayakumari, Demonstration of effective acoustic properties of different configurations of Helmholtz resonators, *Applied Acoustics*, vol. 155, pp. 371–382, 2019.
- [6] S. Kumar, T. B. Xiang, and H. P. Lee, Ventilated acoustic metamaterial window panels for simultaneous noise shielding and air circulation, *Applied Acoustics*, vol. 159, p. 107088, Feb. 2020.
- [7] S. H. Kim and S. H. Lee, Air transparent soundproof window, *AIP Advances*, vol. 4, no. 11, 2014.
- [8] J. W. Jung, J. E. Kim, and J. W. Lee, Acoustic metamaterial panel for both fluid passage and broadband soundproofing in the audible frequency range, *Applied Physics Letters*, vol. 112, no. 4, 2018.
- [9] M. R. Stinson, The propagation of plane sound waves in narrow and wide circular tubes, and generalization to uniform tubes of arbitrary cross sectional shape, *The Journal of the Acoustical Society of America*, vol. 89, no. 2, pp. 550–558, Feb. 1991.
- [10] C Zwikker; Cornelis Willem Kosten, *Sound absorbing materials*. Elsevier Pub. Co., 1949.
- [11] C. Cai and C. M. Mak, Hybrid noise control in a duct using a periodic dual Helmholtz resonator array, *Applied Acoustics*, vol. 134, no. January, pp. 119–124, May 2018.
- [12] U. Ingard, On the Theory and Design of Acoustic Resonators The Journal of the Acoustical Society of America, *The Journal of the Acoustical Society of America*, vol. 25, no. 6, pp. 1037–1061, 1953.
- [13] N. Jiménez, V. Romero-García, V. Pagneux, and J.-P. Groby, Rainbow-trapping absorbers: Broadband, perfect and asymmetric sound absorption by subwavelength panels for transmission problems, *Scientific Reports*, vol. 7, no. 1, p. 13595, Dec. 2017.
- [14] S. Wei, L. Li, C. Zhigang, L. Linyong, and F. Xiaopeng, A parameter design method for multifrequency perfect sound-absorbing metasurface with critical coupled Helmholtz resonator, *Journal of Low Frequency Noise Vibration and Active Control*, no. 174, 2021.
- [15] V. Romero-García, G. Theocharis, O. Richoux, and V. Pagneux, Use of complex frequency plane to design broadband and sub-wavelength absorbers, *The Journal of the Acoustical Society of America*, vol. 139, no. 6, pp. 3395–3403, 2016.
- [16] B. Z. Cheng, N. Gao, R. H. Zhang, and H. Hou, Design and experimental investigation of broadband quasi-perfect composite loaded sound absorber at low frequencies, *Applied Acoustics*, vol. 178, p. 108026, 2021.
- [17] H. Long *et al.*, Tunable and broadband asymmetric sound absorptions with coupling of acoustic bright and dark modes, *Journal of Sound and Vibration*, vol. 479, p. 115371, 2020.
- [18] C. Cai and C. M. Mak, Acoustic performance of different Helmholtz resonator array configurations, *Applied Acoustics*, vol. 130, no. August 2017, pp. 204–209, 2018.
- [19] C. Cai, C. M. Mak, and X. Wang, Noise attenuation performance improvement by adding Helmholtz resonators on the periodic ducted Helmholtz resonator system, *Applied Acoustics*, vol. 122, pp. 8–15, 2017.